THE ACE-CRIS SCINTILLATING OPTICAL FIBER TRAJECTORY (SOFT) DETECTOR: CALIBRATIONS AT THE NSCL AND GSI

P. L. Hink[1], W. R. Binns[1], A. C. Cummings[2], M. A. Lijowski[1], R. A. Mewaldt[2], M. A. Olevitch[1], E. C. Stone[2], T. T. von Rosenvinge[3], and M. E. Wiedenbeck[4]

[1]*Washington University, Campus Box 1105, St. Louis, MO, USA*
[2]*California Institute of Technology, Mail Stop 220-47, Pasadena, CA, USA*
[3]*NASA / Goddard Space Flight Center, Code 661, Greenbelt, MD, USA*
[4]*Jet Propulsion Laboratory, Mail Stop 169-327, 4800 Oak Grove Drive, Pasadena, CA, USA*

ABSTRACT

The Scintillating Optical Fiber Trajectory (SOFT) detector, the hodoscope for the Cosmic Ray Isotope Spectrometer (CRIS) on the NASA Advanced Composition Explorer, was calibrated using 155 MeV/n He, Li, C, N, O, and Ar at the Michigan State University National Superconducting Cyclotron Laboratory (NSCL), and 200 - 700 MeV/n C, Si, and Fe at the GSI facility in Darmstadt, Germany. The flight instrument consists of three hodoscope fiber planes and one trigger plane, read out by an image intensified CCD camera system and by intensified photodiodes respectively. The spatial and angular resolution of the hodoscope is described, along with the detection efficiency of both the hodoscope and trigger plane as a function of charge.

INTRODUCTION

The CRIS instrument is designed to measure the isotopic abundances of the galactic cosmic rays with atomic number $3 \leq Z \leq 30$ and energy $50 \leq E(MeV/n) \leq 500$ (see paper OG 10.2.20). The CRIS instrument utilizes silicon detectors and a scintillating fiber hodoscope to determine mass using the dE/dx - total-E method. The SOFT detector, the hodoscope for the CRIS instrument, is required to have an angular resolution of 0.1° at Fe, with somewhat less stringent requirements at lower Z. This corresponds to a position resolution of < 130 μm for the geometry of the SOFT detector. The detection efficiency is required to be greater than 50% at Beryllium and greater than 90% for Oxygen. We have previously reported results of a prototype SOFT test (Hink et al. 1995) and preliminary results of a flight SOFT calibration (Hink et al. 1996) indicating that position resolution and detection efficiency requirements would be achieved. Here we present an analysis of calibrations of the flight ACE-CRIS SOFT detector at the NSCL and GSI.

THE SOFT INSTRUMENT

Schematic cross sectional views of the SOFT detector are shown in Figure 1. It consists of a trajectory detector composed of three planes (x,y) of scintillating fibers and a trigger detector composed of one plane of scintillating fibers. The fibers have a 200μm square cross section with a 10μm cladding thickness. Each of the three hodoscope planes and the trigger plane are composed of two layers of orthogonally crossed fibers mounted to a Kapton substrate. The hodoscope fibers are individually coated with a black extra-mural absorber (EMA) to prevent cross-talk between fibers and fiber planes. Both ends of the fiber detectors are formatted into tabs with width ~ 2.4cm. These tabs are coherently stacked to produce ~ 2.4cm x 1.7cm fiber outputs at either end of the detector which are each coupled to an image intensified CCD camera described in Hink et al. (1996). The trigger fiber tabs are formatted onto the same image intensifier as the hodoscope fibers, but are read out with photodiodes rather than the CCD. Only one camera system will be operated during the mission to conserve power.

THE SOFT CALIBRATION

The SOFT detector module was exposed to the particle beams at MSU using a non-flight data system and a scintillation detector for charge determination. A 4.8mm thick lead fiducial mask with 1mm diameter holes drilled on 12.7mm centers covering the full 26cm x 26cm area of SOFT was used on one of the runs to calibrate the position determination made by the hodoscope detector. The image intensifier assembly was cooled to 0°C to minimize dark current in the CCD, dark counts in the image intensifier, and to more accurately reflect the on-orbit temperature of the SOFT detector. The MSU calibration included beams of 155 MeV/n He, Li, C, N, O, and Ar.

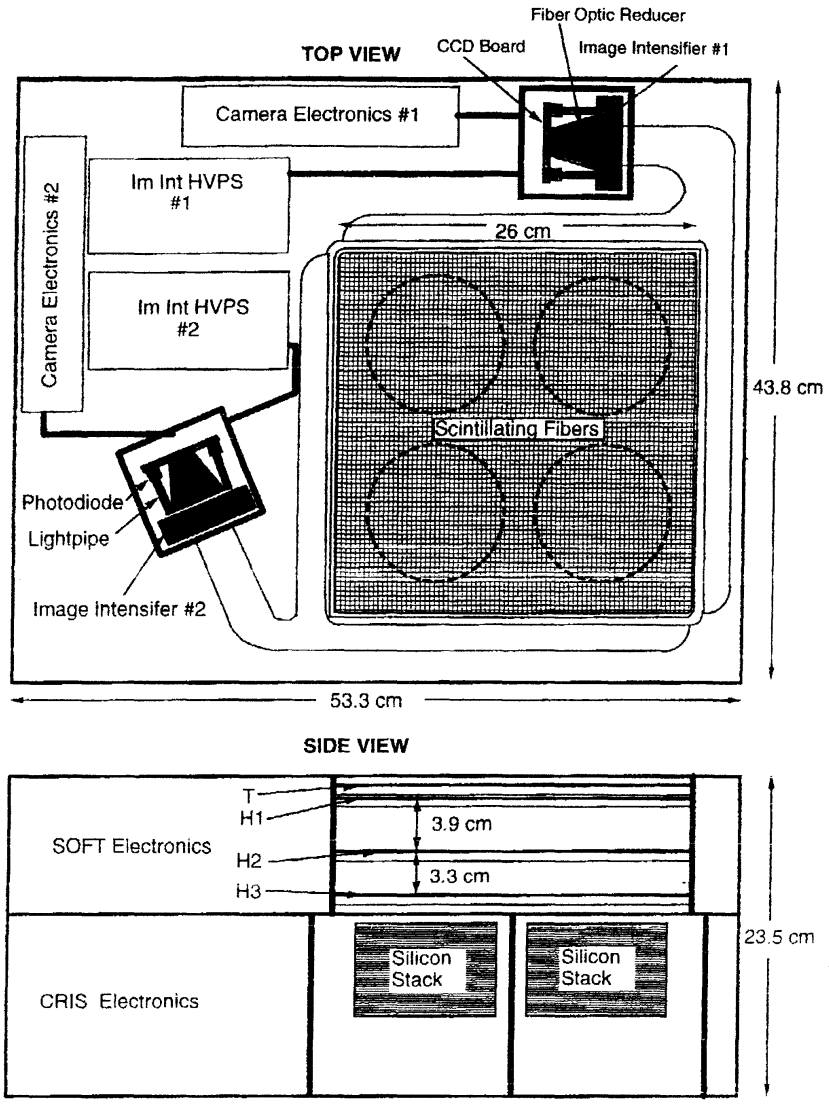

Fig. 1: Schematic of the SOFT detector which consists of three x,y hodoscope planes and a trigger plane. The silicon ddE/dx detectors are directly below the SOFT detector.

The GSI calibration was performed on the full CRIS instrument with a portion of the beam-time devoted to areal and angle calibrations of the SOFT module. The CRIS silicon detectors were used for charge determination. The GSI calibration included beams of 200 - 700 MeV/n C, O, and Fe.

Here we report the following results; 1) an exposure of the full detector area using 155 MeV/n ^{16}O, 2) detection efficiency for 155 MeV/n He, Li, C, N, O, and Ar, 3) trigger plane detection efficiency for 155 MeV/n He, Li, and O, and 4) angular resolution using 700MeV/n Fe. All data presented here were taken with the image intensifier at the default flight gain of 800,000.

RESULTS

Position and Angular Resolution

The SOFT detector position resolution was obtained using the method of residuals (Crary et al. 1992 and Davis et al. 1989). For each event the weighted centroid of each cluster of contiguous pixels in the CCD data was calculated using the CRIS on-board processing algorithm. Each

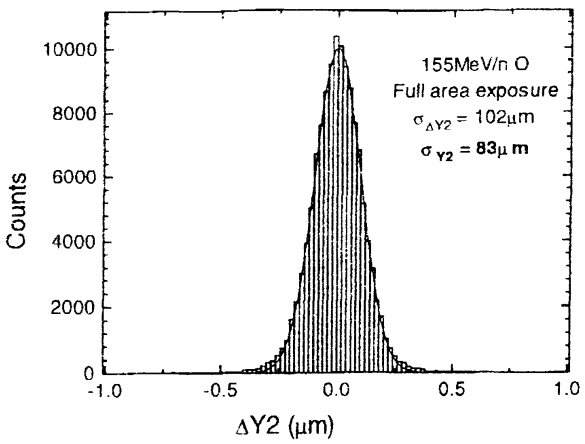

Fig. 2: Position resolution of full SOFT detector using 155MeV/n ^{16}O.

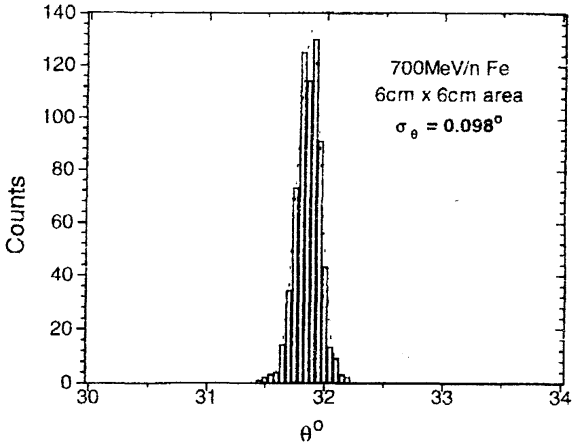

Fig. 3: Angular resolution of 6cm x 6cm region of SOFT detector using 700MeV/n ^{56}Fe.

centroid in the event is assigned to a fiber and layer using a pixel-to-fiber look-up table, retaining precision of 0.125 fiber widths. The real space position is then found by using the fiducial mask data to transform the fiber coordinates into x,y real space coordinates. In Figure 2 we histogram the position resolution of hodoscope layer Y2 using the method of residuals. The data were obtained from the full area map using 155 MeV/n ^{16}O incident at 0°. This resolution is representative of what should be obtained in flight. The 83μm resolution is well within the required 130μm resolution, and approaches the 70μm resolution obtained for a small region (2cm x 2cm) using the same beam. All 6 elements had small region position resolution of better than 110μm.

In Figure 3 we present the angular resolution obtained for 700MeV/n Fe incident at 32° covering a 6cm x 6cm region of the SOFT hodoscope. A first-order correction for beam divergence has been applied to this data. The angular resolution, 0.098°, is consistent with the required resolution even without z-axis variation corrections.

Hodoscope Detection Efficiency

The detection efficiency of the hodoscope was measured for all 6 elements obtained at MSU. The incident angle of the beam was 15° x 15° with respect to the x and y fibers, and nominal flight gains and CCD threshold settings were used. The only selection used to form the detection efficiency data set was a charge cut on the scintillation counter. For each element a data set of roughly 3000 events was obtained. For each event we applied the CRIS on-board algorithm to the SOFT data stream, yielding the centroids of the brightest cluster in each of the 6 layers, plus the next 6 brightest clusters independent of layer. Only events having good straight-line fits using one centroid in each of the 6 layers were considered detected, and the ratio of this to the total number of events in the data set is defined as the 6 layer detection efficiency, η_{DE}. In flight, we may accept events with missing layers if additional criteria are met, so the actual efficiency may be better than that presented here. In Figure 4 we plot the detection inefficiency ($1 - \eta_{DE}$) for all 6 elements. We find that both of the SOFT camera systems meet the detection efficiency requirements for Be (>50%) and O (>90%). The detection efficiency is expected to depend on energy, as dE/dx does. Since most stopping Be and all stopping He in CRIS have energies < 155 MeV/n, the detection efficiencies for these light elements should be higher than depicted in Figure 4. We also find that camera 2, however, is significantly better than camera 1. This is probably a result of differences in the fiber-optic faceplate used on the image intensifiers (Hink et al. 1996). We plan to use camera 2 as the default camera for the mission.

Trigger Detection Efficiency

In normal operation the logical OR of the two trigger planes is used along with signals from the CRIS silicon stack detectors to form coincidence. To determine the detection efficiency of the trigger planes we monitored the trigger signals from each plane on each camera during portions of the MSU calibration. Data sets were formed by making charge cuts based on the scintillation counter, as described above. The detection efficiency is defined as the fraction of events in this data set that detected the particle in at least one of the trigger planes. The efficiencies were quite high, with 100% detection efficiency for both camera 1 and 2 using 155 MeV/n ^{16}O. Camera 2 had better efficiency at lower charges, 99.8% at Be and 93.5% at He, as compared to camera 2, 97.3% at Be and 75.1% at He. This is consistent with the higher detection efficiencies found in the camera 2 hodoscope.

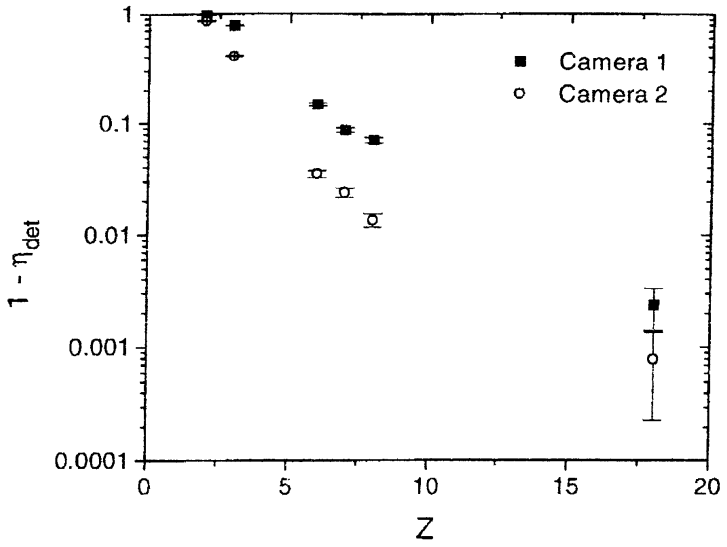

Fig. 4: The SOFT hodoscope detection inefficiency (1 - η_{DE}) vs. atomic number (Z) for 155 MeV/n particles.

CONCLUSIONS

We have determined that the position resolution of the flight ACE-CRIS hodoscope over its full area is better than the 130μm required. We have also demonstrated the required angular resolution over a smaller portion of the detector. The 6 layer detection efficiency for both cameras is within the requirements of 50% for Be and 90% for O. The trigger planes have detection efficiencies much better than this as anticipated.

ACKNOWLEDGEMENTS

This work was supported in part by NASA contract NAS5-32626, other NASA grants, and in part by the McDonnell Center for the Space Sciences at Washington University.

REFERENCES

Von Rosenvinge, T. T., Allbritton, G., Binns, W. R., et. al., *Proc. 25th ICRC*, OG 10.2.20 (1997).
Crary, D. J., et. al., *Nuclear Instruments and Methods*, **A316,** 311 (1992).
Davis, A. J., Hink, P. L., Binns, W. R. et. al., *Nuclear Instruments and Methods*, **A276,** 347 (1989).
Hink, P. L., Beatty, J. J., Binns, W. R., et. al., *Proc. 24 Intl. Cos. Ray Conf.* **3**, 653 (1995).
Hink, P. L., Binns, W. R., Klarmann, J., et. al., *SPIE*, **2806**, 199 (1996).